2020 Numisheet benchmark study tension/compression test summary

William E. Luecke Evan Rust Mark A. Iadicola*

2020-03-27

1 Introduction

This report describes the test equipment, process, analysis, and data-file formats for the tension/compression testing of the four materials associated with the Numisheet conference Benchmarks. The four materials include two steels alloys, DP980 for Benchmark 1 and DP1180 for Benchmark 2, and two 6000 series aluminum alloys, AA6xxx-T4 for Benchmark 1 and AA6xxx-T81 for Benchmark 2, that will be referred to here as BM1-DP980, BM2-DP1180, BM1-6xxx-T4, and BM2-6xxx-T81, respectively. The testing reported here was requested by the 2020 Numisheet Benchmark Committee and was performed by the National Institute of Standards and Technology (NIST) Center for Automotive Lightweighting (NCAL) in Gaithersburg, MD.

This data can be found using digital object identifier doi:10.18434/M32202.

2 Test Methods

2.1 Specimen

Figure 1 shows the tension/compression specimen, which was fabricated using commercial waterjet-cutting equipment. Reported thickness and width dimensions are the average of three measurements made on the center and at each end of the reduced parallel section of the test specimen. The edge of the specimen that was patterned for digital image correlation was finished with 600-grit grinding paper, but the opposite edge was left as cut. All specimens were oriented at 0° to the rolling direction, but future tests will include other orientations.

*Please direct all questions regarding this data and report to Mark Iadicola: mark.iadicola@nist.gov.

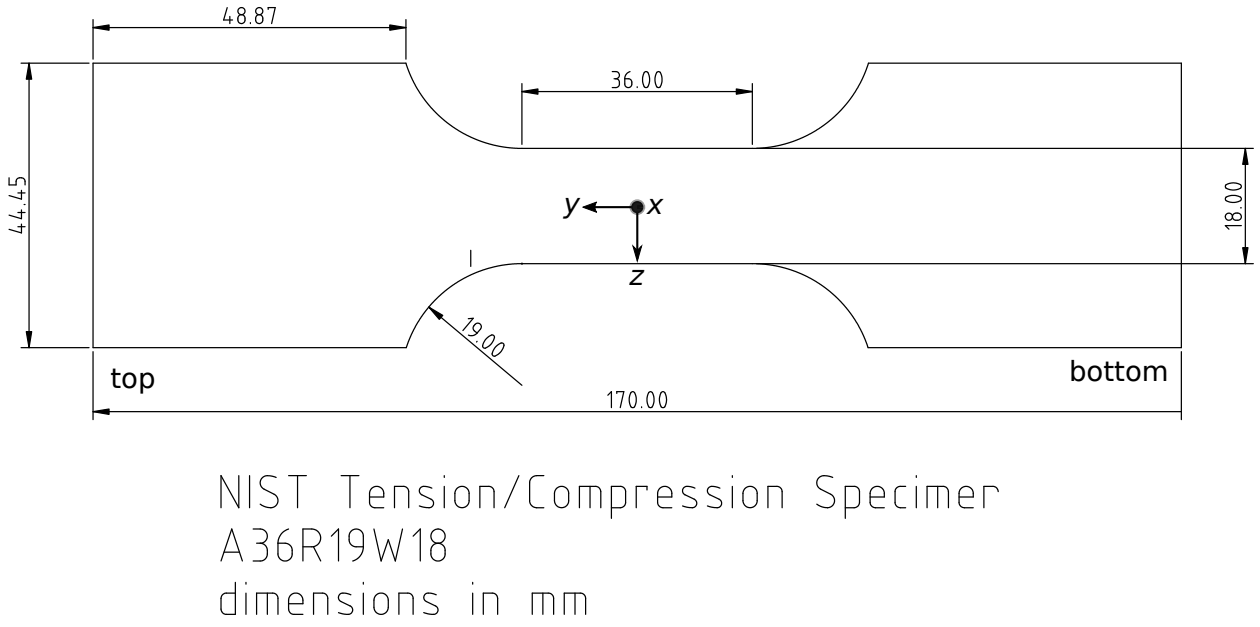

Figure 1: NIST tension/compression specimen.

2.2 Mechanical testing equipment

Figure 2 shows the testing machine, the locations of the upper and lower load cells, and the pneumatic actuators that apply the forces to the anti-buckling fixture. The anti-buckling force actuators are attached to the columns of the testing machine, and do not move with the specimen. A load cell in each anti-buckling force actuator measures the applied force. The testing machine alignment met ASTM E1012 Class 5 [1], and the protocol and anti-buckling fixture meet the requirements for qualifying for sheet compression testing using ASTM E9 [2]. Figure 3 shows the anti-buckling fixture. To reduce friction, the faces that touch the test specimen were covered with a polytetrafluoroethylene (PTFE) adhesive film 0.13 mm thick, and then further lubricated with petroleum jelly. In its central section, the test specimen projects 1 mm from the anti-buckling fixture.

2.2.1 Test Protocol

Each test consisted of six segments.

1. After a short ramp in force control brought the specimen to zero force, the operator initiated the image acquisition, and then a few seconds later, the displacement-control ramp described as segment 2.

2. The actuator moved in tension in displacement control to a fixed displacement determined

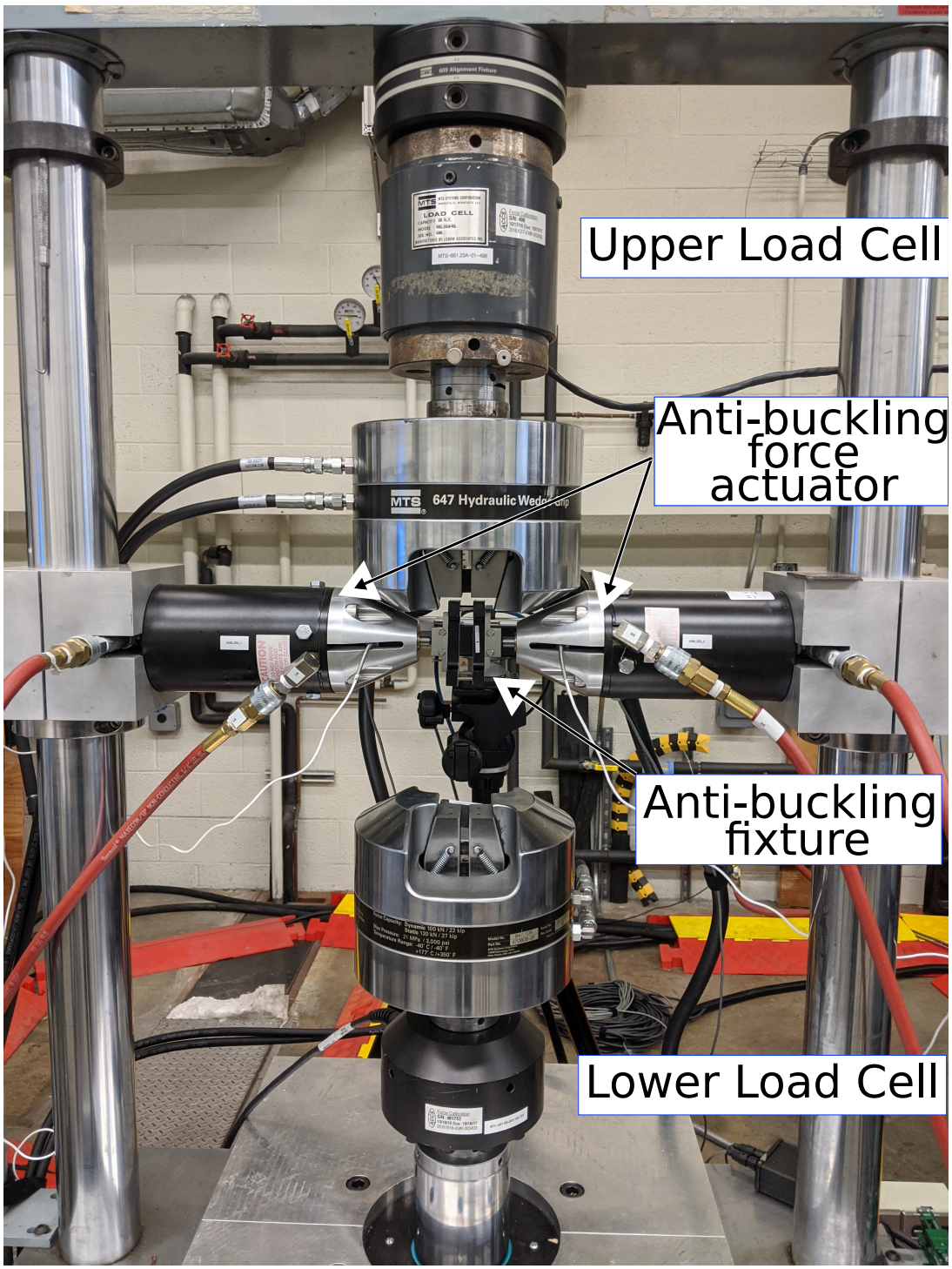

Figure 2: NIST tension/compression testing machine.

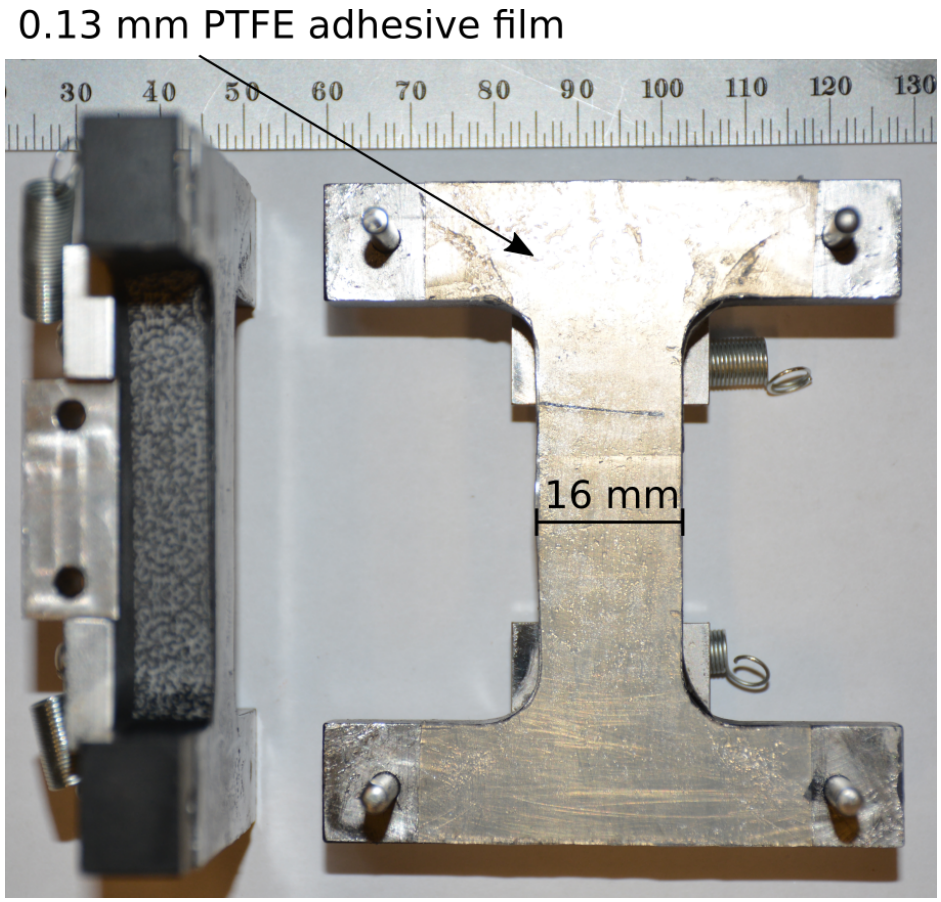

Figure 3: Anti-buckling fixture.

to produce a nominal engineering strain about 75 % of the uniform engineering strain.

3. The actuator held for 10 s in displacement control.
4. The actuator moved in compression in displacement control to a fixed displacement determined to produce a final specimen engineering strain approximately zero.
5. The actuator held for 10 s in displacement control.
6. The actuator moved in tension in displacement control until the specimen failed.

The entire test took place with the anti-buckling fixture in contact with the specimen and the full 3000 N force applied. In some tests the image acquisition rate was 4 images per second during the elastic loading and unloading segments, which was then reduced to 1 image per second for the plastic portions.

Test parameters

- Actuator velocity: 0.54 mm/min
- Nominal engineering strain rate : 0.015 mm/mm/min = 0.00025 mm/mm/s (ASTM E8 standard rate)
- Force was defined as the average of the upper and lower load cells. Typically the difference between the upper and lower load cell was less than 300 N.
- The anti-buckling force was set to 3000 N at the start of the test and not adjusted. Typically it varied by less than 300 N during the course of the test.
- Three tests were repeated for each material.
- The tests took place at NCAL from October, 2019 through January, 2020.

2.3 DIC test equipment and analysis

The local true strains in the test specimen were measured using digital image correlation (DIC) from a pattern applied to the thickness dimension of the test specimen. The pattern was a white spray-painted base oversprayed with black spots. Table 1 summarizes the DIC hardware for the six tests, as recommended in Reference [3]. A separate sensitivity study, Appendix 4.1, yielded optimal DIC analysis parameters for all tests: Subset size = 17 pixels, Step size = 7 pixels, Strain-filter size = 5 pixels. For the hardware parameters in Table 1, with image scale 52.6 pixel/mm, the virtual strain gauge size, defined in Eq. (1), corresponds to 45 pixels = 0.86 mm, and represents the effective length over which local true strains are measured. The noise-floor analysis, Appendix 4.2, yielded an estimate of the uncertainty of a local true ε_{yy} strain measurement to be 291 μm/m .

Table 1: Summary of DIC hardware, setup, and analysis used in DIC acquisitions.

Item	Value
Configuration ID	[CD191118-WEL-001]
Cameras	PGR-GS3-U3-91S6M- C13306294 and -C16138026 Point Gray Research Grasshopper 3 camera 9.1 MP, Sony IcX814CCD 1 in. 3.69 μmpitch, 3376x2704 9 FPS
Lenses	Tokina AT-X 100mm macro lens f/2.8 0.3m minimum focusing distance, 55mm filter 7264245 and 7264422
FOV	51 mm x 64 mm ($w \times h$) based on image magnification
Standoff	640 mm
Stereo angle	22.495° $\pm$ 0.005° (range of all calibrations)
Image scale	52.6 pixel/mm (typical value)
Aperture	f8
Image acquisition rate	Noise floor (Sec. 4.2): 250 ms between images
Image acquisition rate	Test: 250 ms initially, then 1 s after yield
Exposure time	5 ms (typical)
Lighting	white light-emitting diode [NCAL-LED-2]
Camera interface	USB-3
Software	Correlated Solutions `Vic-3D` 8.2.4 build 525.
	Affine subset shape function
	True (Hencky) strain calculation

Notes.

- In this report NCAL unique identifiers are typeset in sans serif font surrounded by brackets, such as [CD191118-WEL-001]. These identifiers are included so that any inquiries can be efficiently traced back to the raw data and configurations.

- Certain commercial equipment, instruments, or materials are identified in this paper in order to specify the ex- perimental procedure adequately. Such identification is not intended to imply recommendation or endorsement by the National Institute of Standards and Technology, nor is it intended to imply that the materials or equipment identified are necessarily the best available for the purpose.

The engineering stress-strain diagrams shown in Section 3 were created by defining a virtual extensometer with nominal gauge length of of $G = 22.7$ mm (BM2-DP1180) or $G = 23.6$ mm (others), centered on the reduced parallel length of the specimen to within ± 0.5 mm using alignment marks on the specimen and fixture. In all analyses, the coordinate system is centered on the midline of the thickness of the specimen, and at the y center of the reduced parallel length.

Figure 4 shows a typical analysis of the ε_{yy} true strain distribution at a single point along the area of interest, and the relation of the area of interest (AOI) to the length of the specimen. The colors designate different contours of true strain. The AOI encompasses the entire reduced parallel section of the test specimen plus a length of about a millimeter into each fillet. In all files, the x direction is horizontal, that is across the thickness of the test specimen. The y direction is vertical, that is the tensile axis. The output of each test is a true strain profile with interpolated estimates of the local centerline true strain at each individual time step. These strain profiles contain 145 deformed coordinate and strain points (reduced parallel length, $A = 36$ mm, with interpolated points spaced 0.25 mm apart, from an area of interest centered as closely as visually possible on the center of the specimen.) They were produced using the Correlated Solutions `Vic-3D` "Export metric node data" function.

3 Analysis

3.1 Engineering stress-strain diagrams

This section contains engineering stress-strain diagrams for the four materials at two strain scales:

Material	Full	Low-strain
BM2-DP1180	Fig. 5	Fig. 6
BM1-DP980	Fig. 7	Fig. 8
BM2-6xxx-T81	Fig. 9	Fig. 10
BM1-6xxx-T4	Fig 11	Fig. 12

3.1.1 Comments

The small strain offsets during the compression segment of the tests are artifacts caused by programming the tests in displacement control, rather than in strain control. Each test ran to a fixed tensile displacement before reversing, so displacements such as different seating of the grip wedges, slight unbending of the specimen, or different initial micrometer-scale slipping of the teeth of the wedges cause the specimen to achieve slightly different strains at reversal for the same actuator displacement.

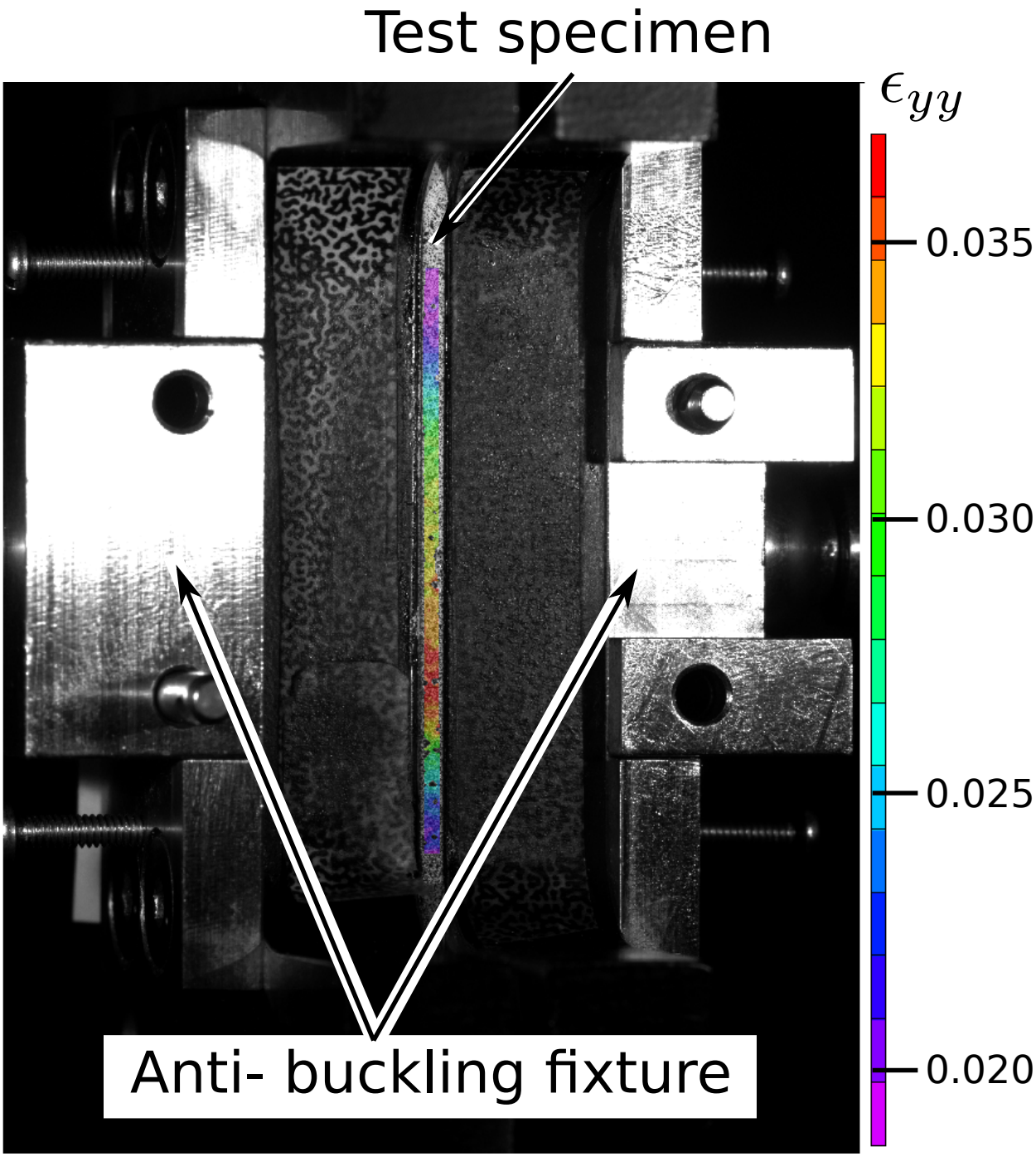

Figure 4: ε_{yy} (true) strain (in mm/mm) distribution from a typical BM1-DP980 test [E191120-WEL-002]. At this point in the test, the specimen is in the second tension segment and has necked. The y direction is positive vertical.

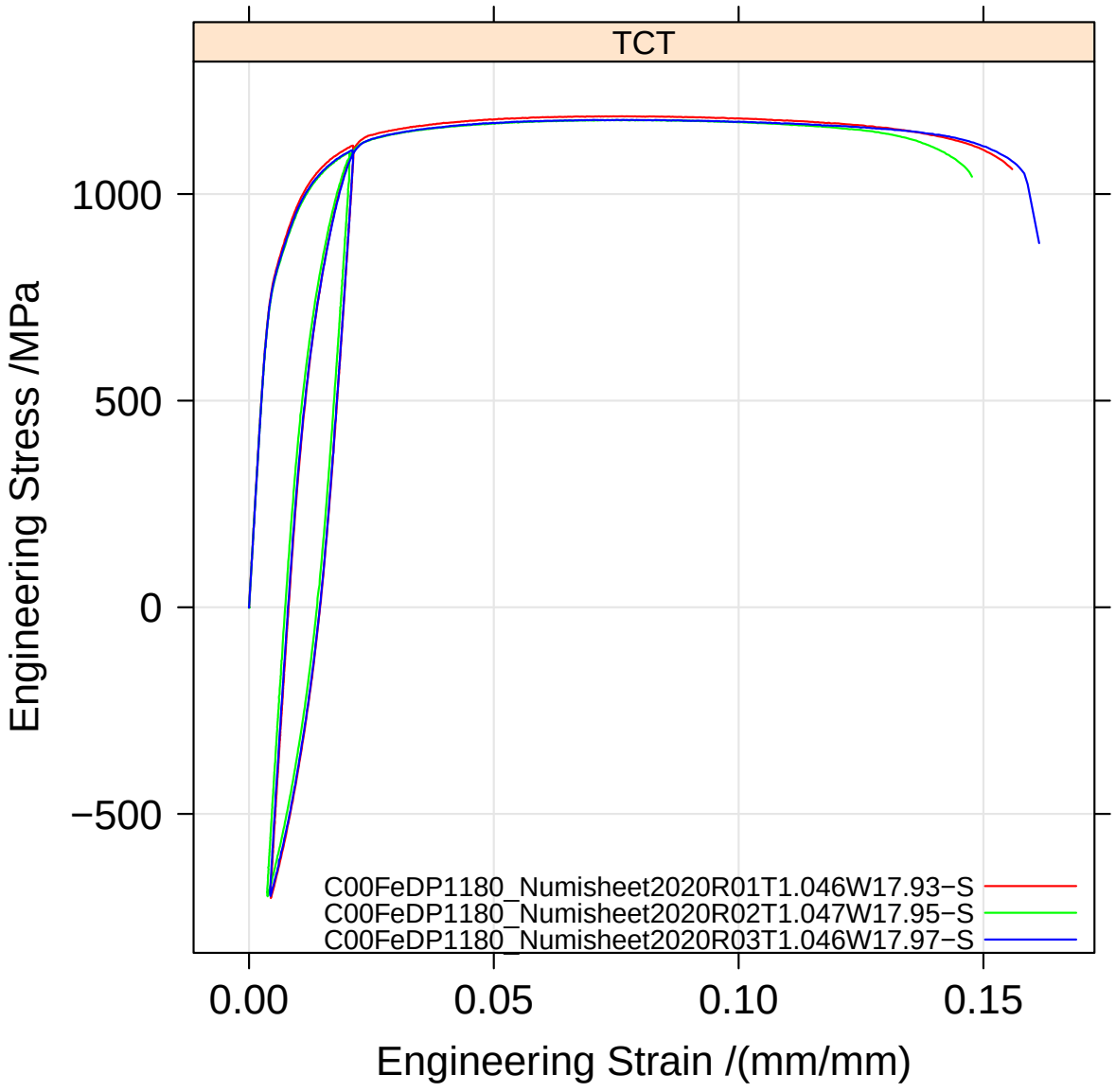

Figure 5: Engineering stress-strain diagram for Benchmark tests of BM2-DP1180.

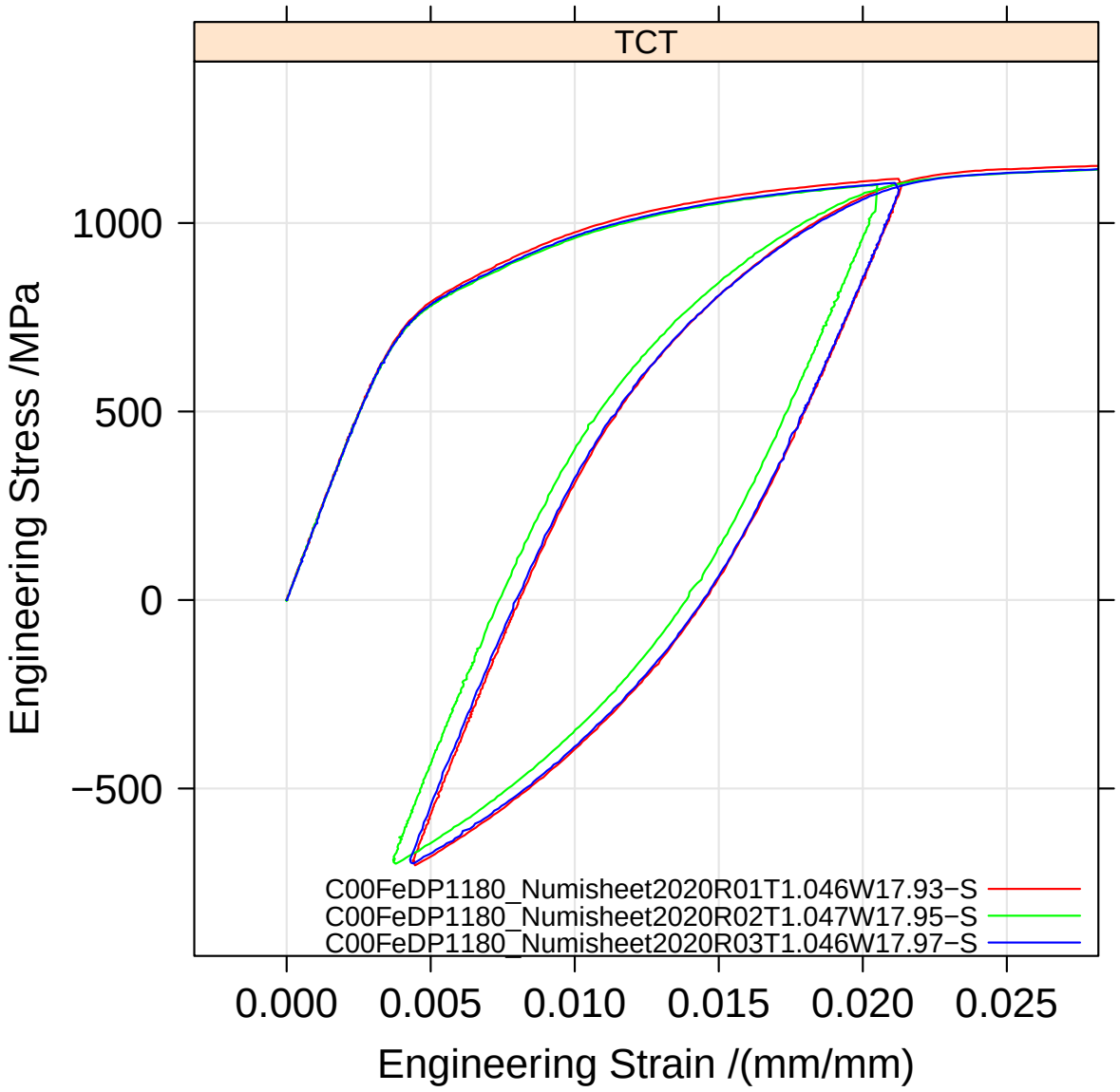

Figure 6: Engineering stress-strain diagram for Benchmark tests of BM2-DP1180 in the low-strain region.

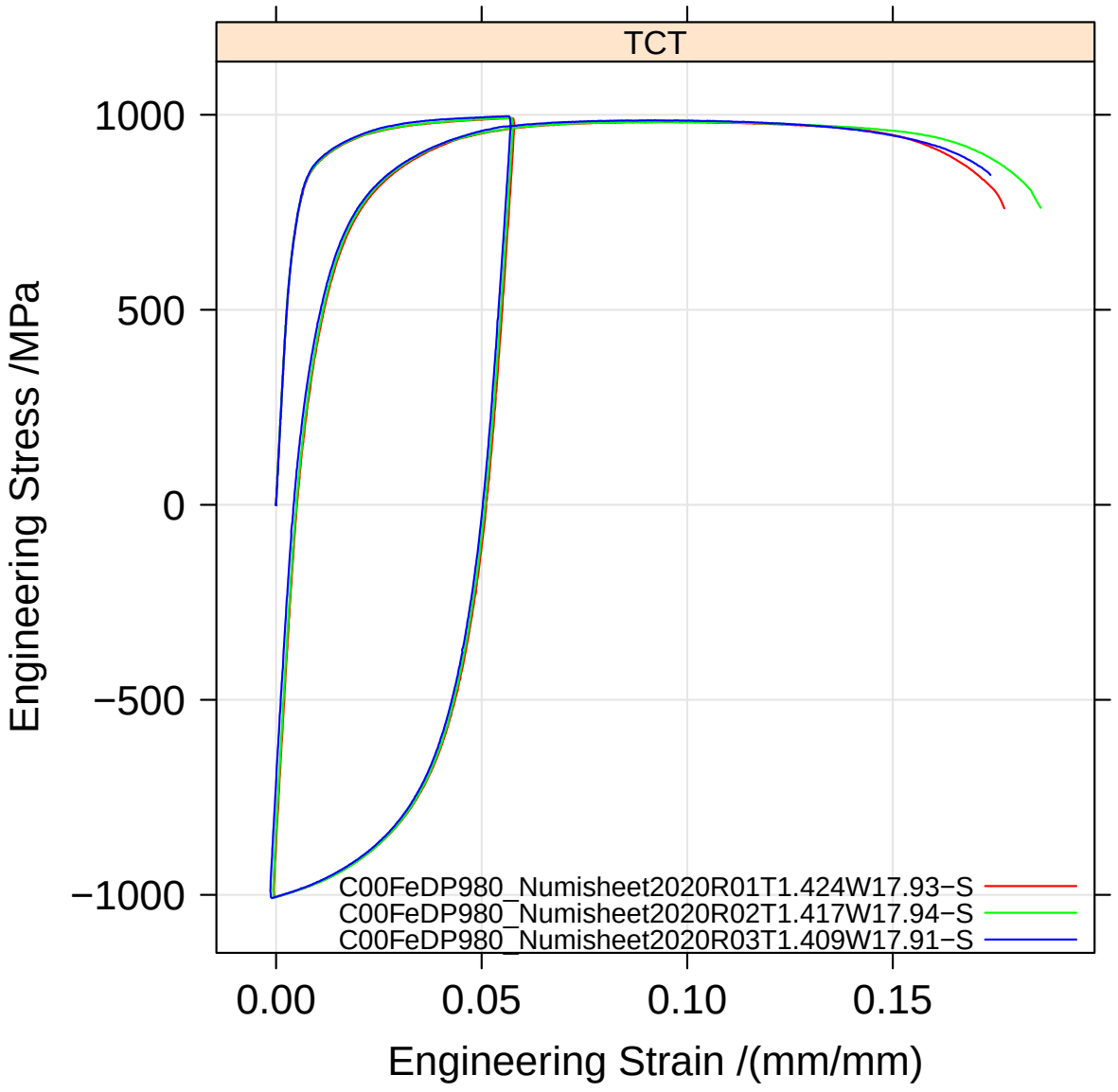

Figure 7: Engineering stress-strain diagram for Benchmark tests of BM1-DP980.

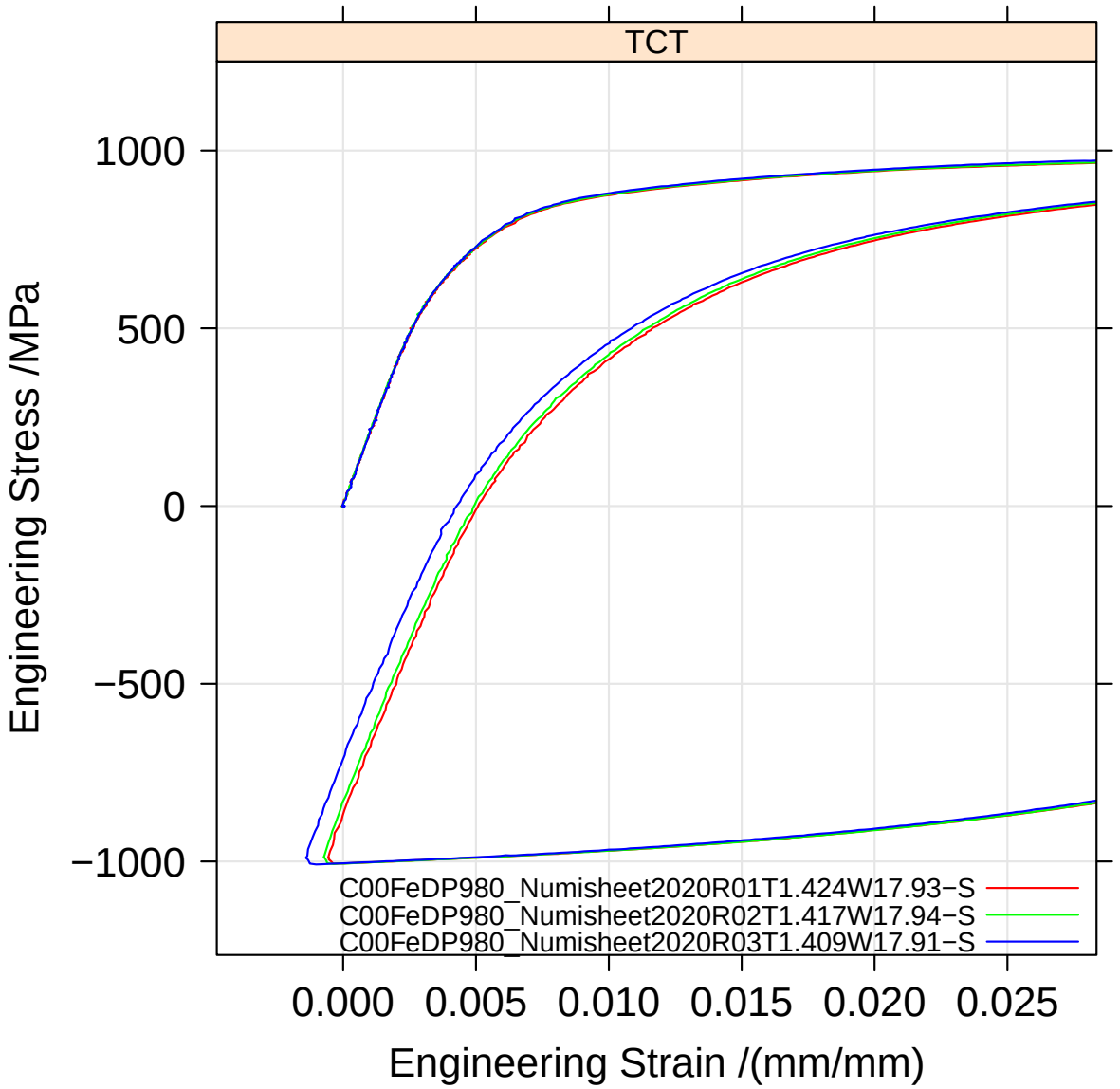

Figure 8: Engineering stress-strain diagram for Benchmark tests of BM1-DP980 in the low-strain region.

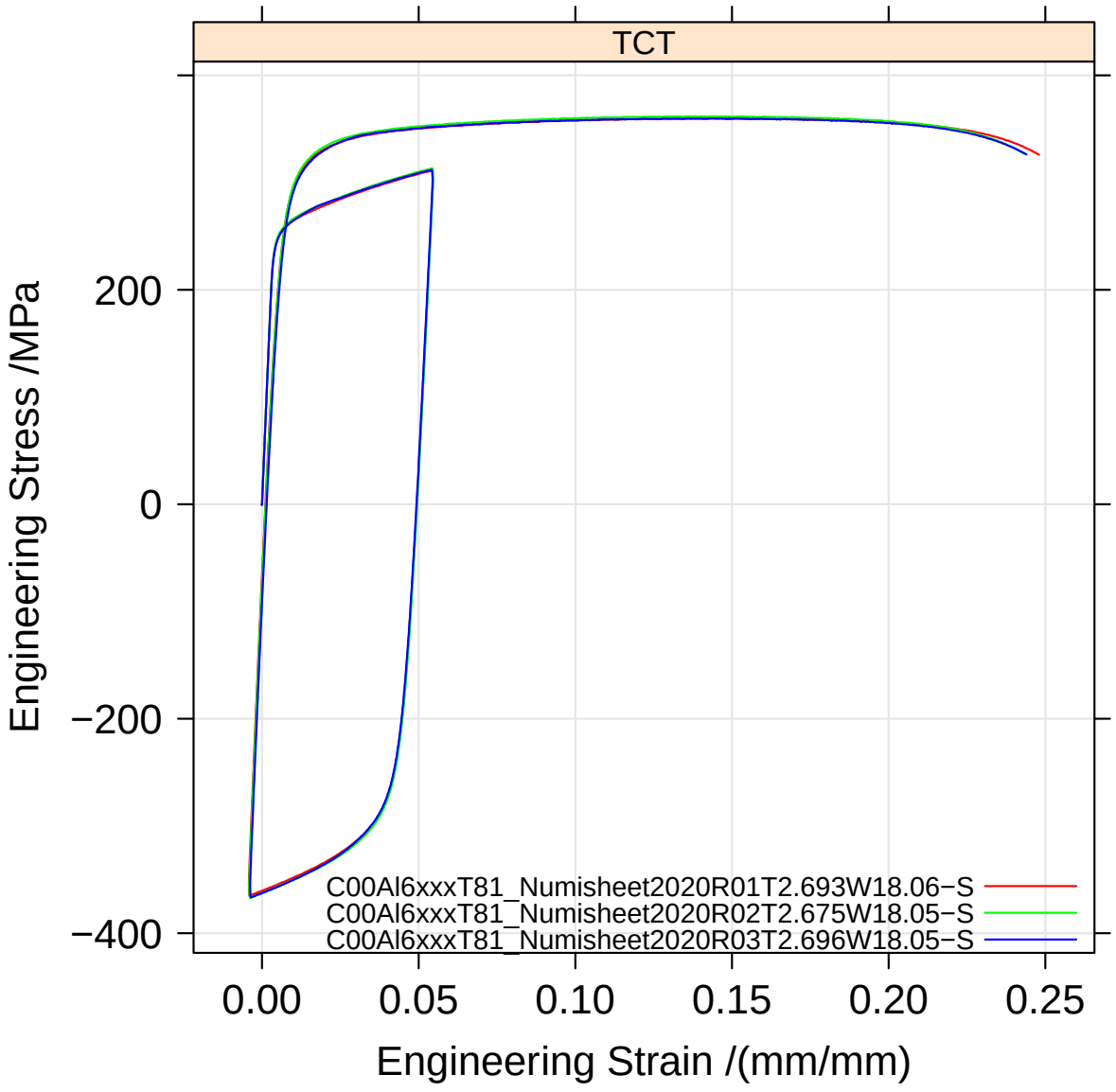

Figure 9: Engineering stress-strain diagram for Benchmark tests of BM2-6xxx-T81.

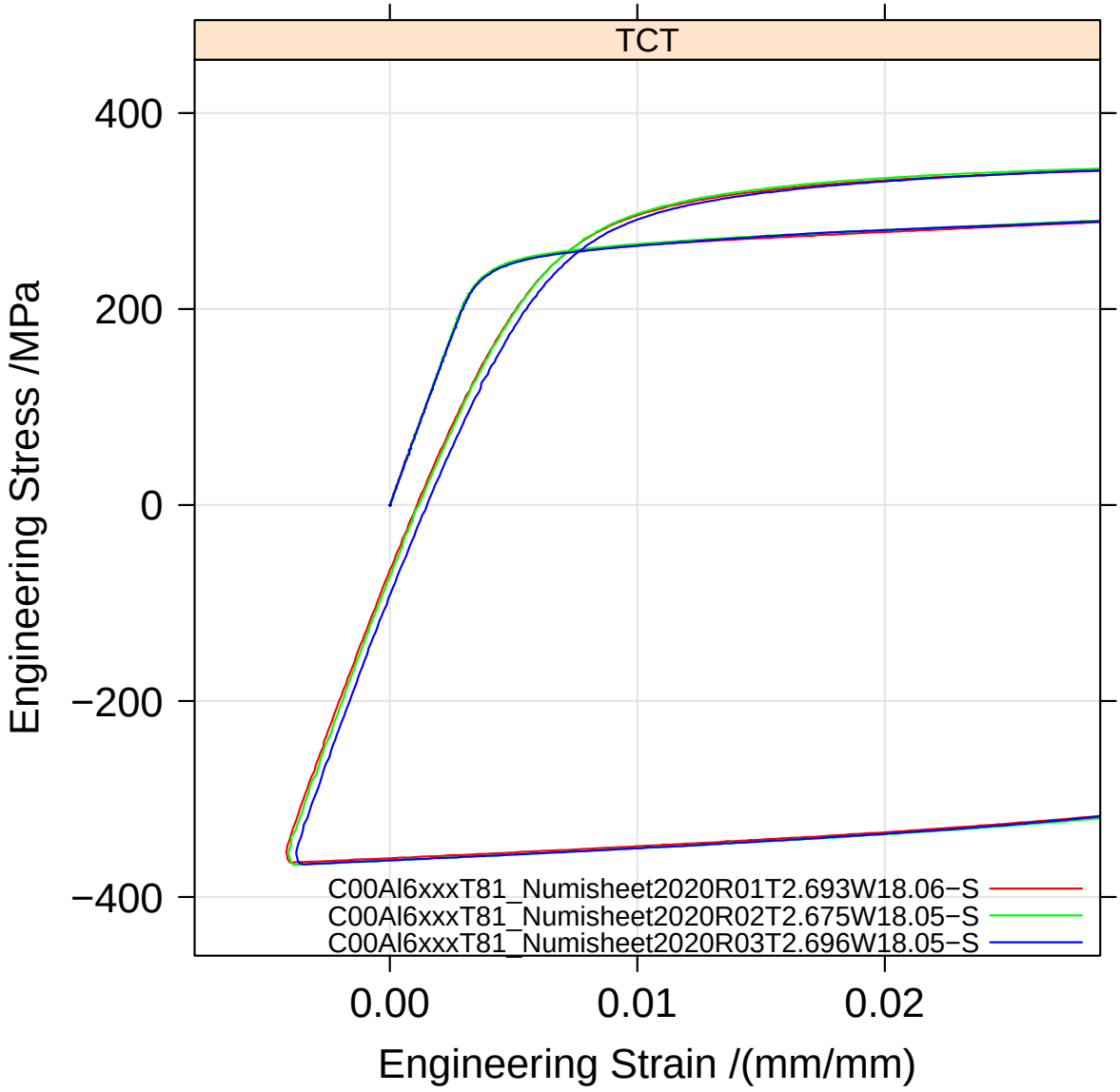

Figure 10: Engineering stress-strain diagram for Benchmark tests of BM2-6xxx-T81 in the low-strain region.

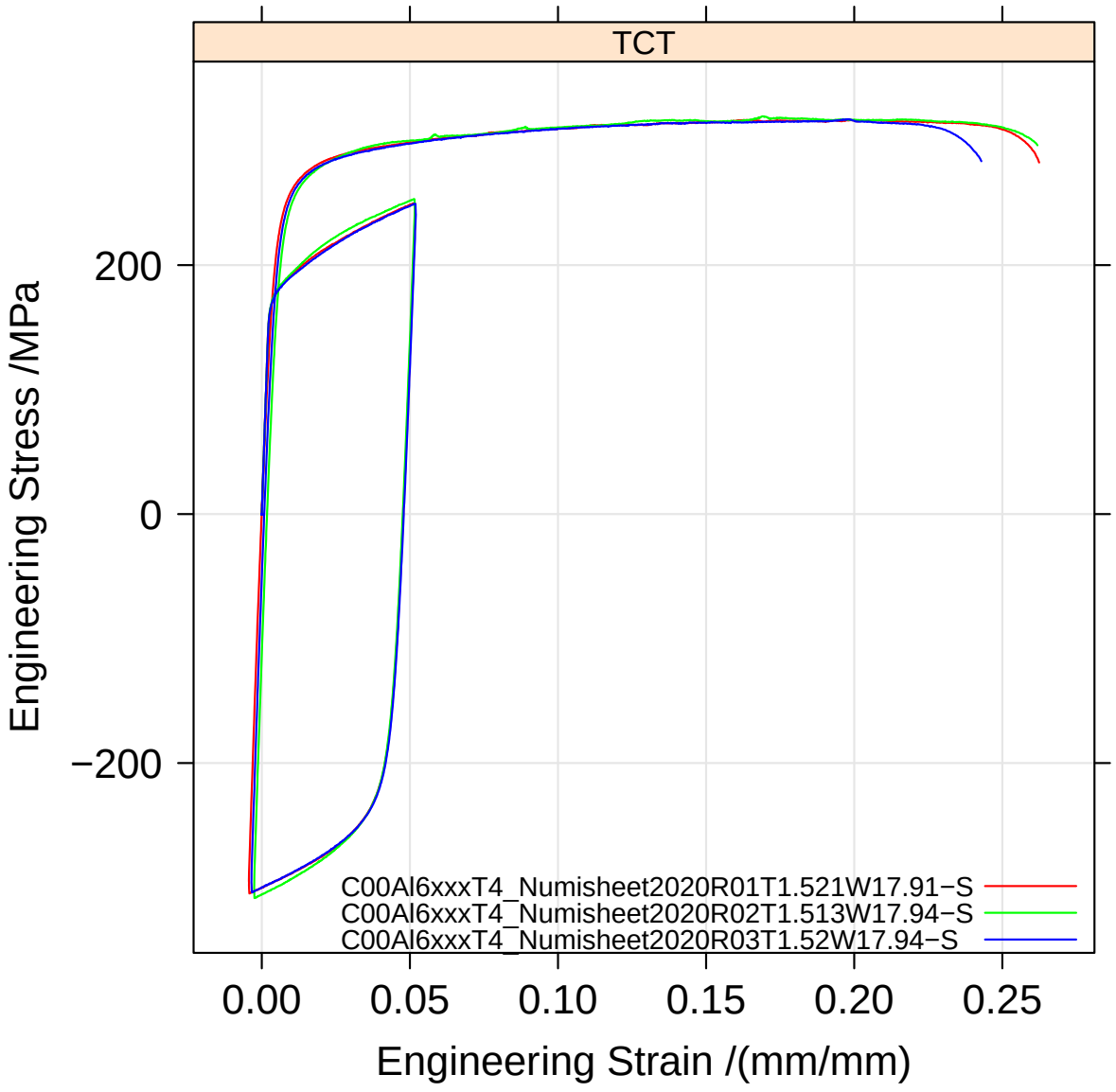

Figure 11: Engineering stress-strain diagram for Benchmark tests of BM1-6xxx-T4.

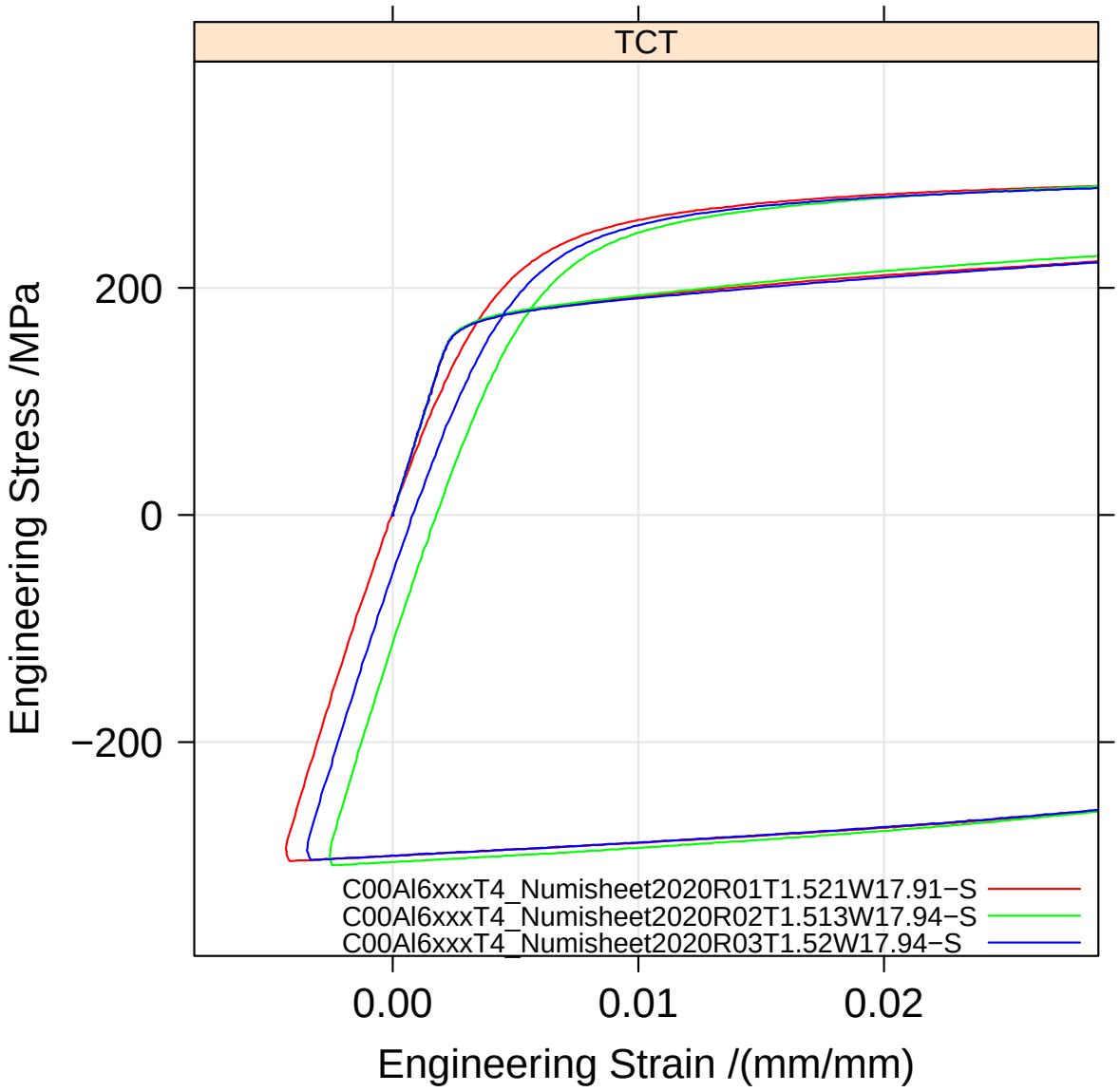

Figure 12: Engineering stress-strain diagram for Benchmark tests of BM1-6xxx-T4 in the low-strain region.

4 Appendixes

4.1 Sensitivity Study

This appendix summarizes the sensitivity study used to determine the optimal digital-image correlation analysis parameters. During the processing of the DIC images the analysis parameters used significantly affect both the noise floor and the maximum measurable gradients of strain and displacement. Since the longitudinal strain, ε_{yy}, is the primary quantity in the representation of the stress-strain response, this quantity of interest will be the focus of the effects of the DIC analysis parameters. The process of selecting an optimal set of DIC analysis parameters is often referred to as a virtual strain gauge (VSG) study, and is described in Reference [3]. The results of the VSG study depend on the hardware and setup of the DIC system and on the DIC pattern used. The virtual strain gauge size, S_{VSG}, in pixels is defined as

$$S_{\text{VSG}} = S_{\text{ss}} + (F-1)S_{\text{st}} \tag{1}$$

where S_{ss} is the subset size, S_{st} is the step size, and F is the strain-filter size for computing the local strains. It represents the length over which local strains are measured. Smaller VSG lengths typically result in a larger strain noise but better-resolved strain gradients, while larger VSG lengths typically result in smaller strain noise but more smoothed strain gradients. An informed balance between the two desirable but competing outcomes (low strain noise versus better-resolved strain gradients) is the goal of the VSG study.

This VSG study used data from NCAL test [E191121-WEL-002], but tests for all four materials used the same hardware, setup, and patterning method, so the results apply to all four materials. It used images 0008 and 1595 of acquisition [E191121-WEL-002-D01], which was analyzed in DIC analysis [E191121-WEL-002-D01-05]. Image 0008 is from the preload phase, with the actuator not moving, while image 1595 is from near failure. Failure began at image 1630, and the specimen broke at image 1644. At this time, the image acquisition rate was 1 Hz, so image 1595 was from 49 s before failure. At the nominal strain rate during the test, $e_{\text{nom}} = 0.00025$ mm/mm/s, this time corresponds to about $e = 1.2$ % nominal engineering strain.

Figure 13 summarizes the sensitivity study. Figure 13a shows the standard deviation of the ε_{yy} strain in the preload phase as a function of VSG size. Figure 13b shows the behavior of the local ε_{yy} true strain along the reduced parallel length near the neck for several different parameter settings. The figure omits virtual strain gage sizes greater than 60 pixels for clarity. Figure 13c plots the peak data from Figure 13b as a function of virtual strain gage size. Figure 13d plots the peak value of the local true strain in the neck against the standard deviation of the ε_{yy} true strain established in the static preload phase, Figure 13a. Larger virtual strain gages reduce the noise, but smooth and reduce the peak strains measured in the neck. In all four plots, the dashed red line indicates the final optimal value, which represents a balance between capturing much of the high strain behavior while restricting the local strain noise.

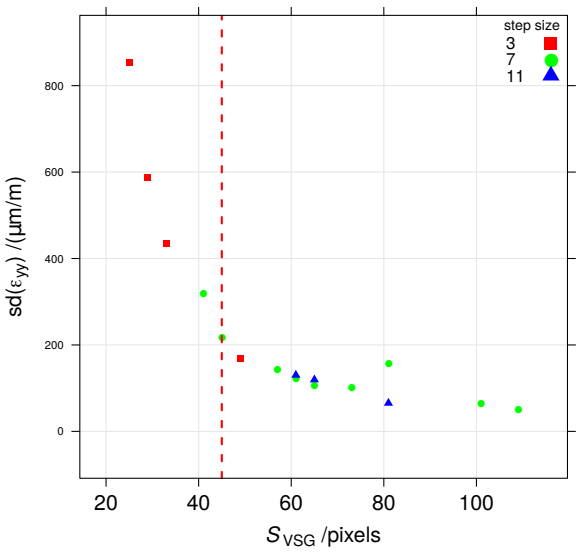

(a) Standard deviation of the ε_{yy} true strain in the AOI during the preload phase.

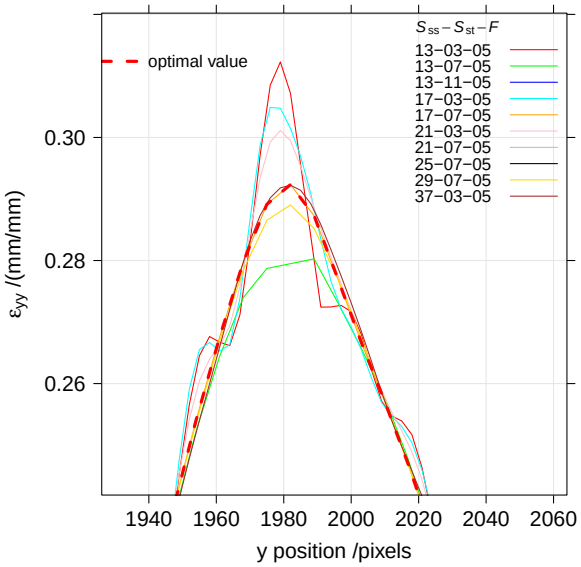

(b) ε_{yy} strains along the centerline of the specimen in the necked region for a variety of subset sizes, step sizes, and strain-filter sizes.

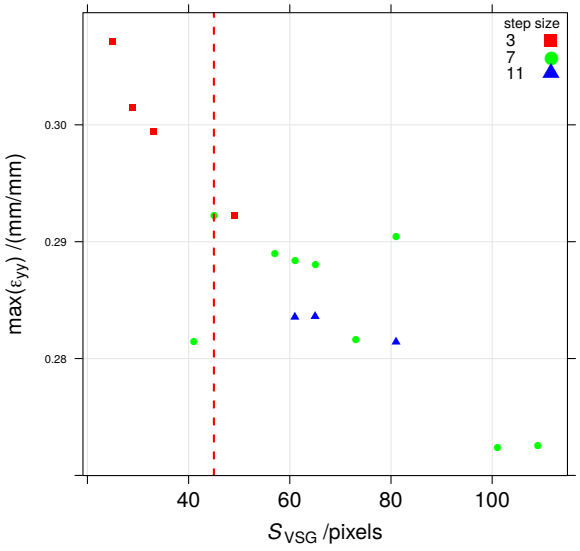

(c) Peak value of the ε_{yy} true strain in the neck as a function of the virtual strain gage size, S_{VSG}.

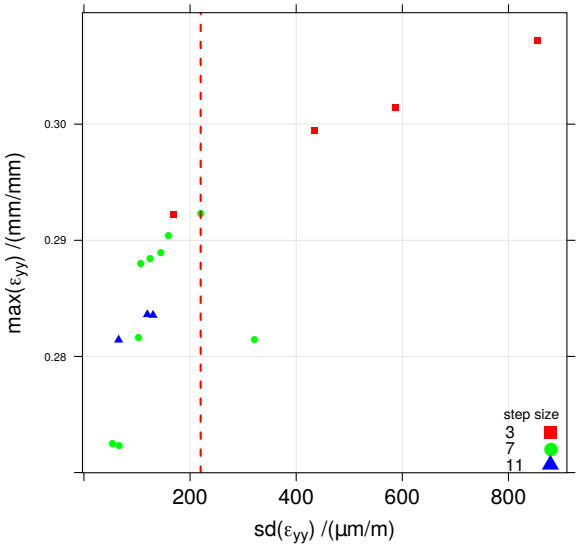

(d) Peak value of the ε_{yy} true strain in the neck as a function of the standard deviation of the ε_{yy} true strain established in the static preload phase.

Figure 13: Virtual strain gage study results. The dashed red line indicates the final optimal value.

4.1.1 Final DIC parameters

Subset size	S_{ss}	17
Step size	S_{st}	7
Strain-filter size	F	5

Based on the selected optimum parameters, strains near $\varepsilon_{yy} = 0.292$ mm/mm should be considered a lower bound of the actual strain in the neck. This analysis is documented as NCAL ID [L191210-WEL-001].

4.2 Noise-floor analysis

At the start of each test, but before any actuator motion, the data acquisition system captured several dozen static images at 250 ms intervals. The first five static images were used to estimate the noise floor for each test, summarized in Table 2. The noise-floor value was used as a simple quality metric to determine if there was any outlier behavior in the DIC system, calibration, or pattering. The ε_{yy} true strain noise floor, $n_{\varepsilon_{yy}}$, reported in Table 2 are the sum of the absolute value

Table 2: Noise-floor estimates for ε_{yy} data.

File	Noise floor μm/m
C00Al6xxxT4_Numisheet2020R01T1.521W17.91-S	251
C00Al6xxxT4_Numisheet2020R02T1.513W17.94-S	229
C00Al6xxxT4_Numisheet2020R03T1.52W17.94-S	253
C00Al6xxxT81_Numisheet2020R01T2.693W18.06-S	234
C00Al6xxxT81_Numisheet2020R02T2.675W18.05-S	296
C00Al6xxxT81_Numisheet2020R03T2.696W18.05-S	232
C00FeDP1180_Numisheet2020R01T1.046W17.93-S	586
C00FeDP1180_Numisheet2020R02T1.047W17.95-S	272
C00FeDP1180_Numisheet2020R03T1.046W17.97-S	363
C00FeDP980_Numisheet2020R01T1.424W17.93-S	263
C00FeDP980_Numisheet2020R02T1.417W17.94-S	256
C00FeDP980_Numisheet2020R03T1.409W17.91-S	258

of the mean value of ε_{yy} and the standard deviation, sd, of ε_{yy} evaluated over the Area of Interest (AOI) for the test:

$$n_{\varepsilon_{yy}} = |\text{mean}(\varepsilon_{yy})| + \text{sd}(\varepsilon_{yy}) \tag{2}$$

The value reported is the worst value from the five images. The majority of the noise floor comes from the spatial variation in ε_{yy} expressed in the standard deviation, rather than from the change in the mean value.

4.3 Naming convention

Strain profiles in comma-separated value file format are named using a convention that encodes the deformation mode, orientation, material, and test specimen dimensions, for example

C00FeDP1180_Numisheet2020R01T1.046W17.93-S.csv

Table 3 explains this naming convention. In addition, this report includes individual files containing traditional stress-strain curves, which are named with the same base naming convention, but have "-Stress-Strain" appended. For complicated compatibility reasons, these filenames omit the "_" characters.

4.4 Data file formats

4.4.1 Format of the summary table file

The tension/compression summary table file (Numisheet2020-tension-compression-summary.csv) contains information about each test including file names, NCAL database identifier, measured geometry, noise floor, and DIC image number of note. See Table 4 for an explanation of each column.

4.4.2 Format of the strain profiles

Six strain profiles are included that contain a strain trace running on the center line of the side of the specimen for each experimental point on the stress-strain curve. Section 4.3 describes the naming convention. The strain profiles were exported using the `Vic-3D` function "export metric node data." The trace of sextuples $(X, Y, Z, \varepsilon_{yy}, \varepsilon_{xx}, \varepsilon_{xy})$ was interpolated for $X = 0$ at 0.25 mm intervals in the range -18 mm $\leq Y \leq +18$ mm, so the file contains

$$(\frac{36 \text{ mm}}{0.25 \text{ mm/point}} + 1) \times 6 \ = \ 870 \text{ columns}$$

of position and strain data. The (X, Y, Z) are the deformed coordinates, and the true strains $(\varepsilon_{xx}, \varepsilon_{yy}, \varepsilon_{xy})$ are the Hencky (true) strains. Following those 870 columns are the raw data captured during the test, summarized in Table 5. Note that the exported interpolated position and strain data are spaced about three times more closely than the virtual strain gauge size, defined in Eq. (1).

4.4.3 Stress-strain file formats

The individual files containing stress-strain curves (Figure 5 through Figure 12) have columns for time, engineering stress and strain, and true stress and strain. They are named using the same base that Table 3 describes. Each stress-strain curve file is accompanied by a separate comma-separated value format file that identifies the data types and units in the columns.

4.5 Data files

4.5.1 Numisheet Benchmark data files

The strain profiles are included with this distribution.

4.5.2 Stress-strain data files

The engineering and true stress-strain data for the Benchmark data are included with the distribution. Engineering stress, S, is calculated as from the instantaneous force, P divided by the original area, A_0.

$$S = \frac{P}{A_0} \tag{3}$$

Engineering strain, e, is calculated from the the original gauge length, L, and the change in gauge length, $L - L_0$.

$$e = \frac{L - L_0}{L_0} \tag{4}$$

True strain, ε, and true stress, σ, are calculated in the usual manner.

$$\varepsilon = \log_e \frac{L}{L_0} = \log_e(1 + e) \tag{5}$$

$$\sigma = S(1 + e) \tag{6}$$

The first-row column headings identify the data. A second file named with "-attributes" appended defines the column names and explains the units of all the files. The files are listed below.

- C00FeDP1180_Numisheet2020R01T1.046W17.93-S
  `C00FeDP1180Numisheet2020R01T1.046W17.93-S-Stress-Strain.csv`
  `C00FeDP1180Numisheet2020R01T1.046W17.93-S-Stress-Strain-attributes.csv`

- C00FeDP1180_Numisheet2020R02T1.047W17.95-S
  `C00FeDP1180Numisheet2020R02T1.047W17.95-S-Stress-Strain.csv`
  `C00FeDP1180Numisheet2020R02T1.047W17.95-S-Stress-Strain-attributes.csv`

- C00FeDP1180_Numisheet2020R03T1.046W17.97-S
  C00FeDP1180Numisheet2020R03T1.046W17.97-S-Stress-Strain.csv
  C00FeDP1180Numisheet2020R03T1.046W17.97-S-Stress-Strain-attributes.csv

- C00FeDP980_Numisheet2020R01T1.424W17.93-S
  C00FeDP980Numisheet2020R01T1.424W17.93-S-Stress-Strain.csv
  C00FeDP980Numisheet2020R01T1.424W17.93-S-Stress-Strain-attributes.csv

- C00FeDP980_Numisheet2020R02T1.417W17.94-S
  C00FeDP980Numisheet2020R02T1.417W17.94-S-Stress-Strain.csv
  C00FeDP980Numisheet2020R02T1.417W17.94-S-Stress-Strain-attributes.csv

- C00FeDP980_Numisheet2020R03T1.409W17.91-S
  C00FeDP980Numisheet2020R03T1.409W17.91-S-Stress-Strain.csv
  C00FeDP980Numisheet2020R03T1.409W17.91-S-Stress-Strain-attributes.csv

- C00Al6xxxT81_Numisheet2020R01T2.693W18.06-S
  C00Al6xxxT81Numisheet2020R01T2.693W18.06-S-Stress-Strain.csv
  C00Al6xxxT81Numisheet2020R01T2.693W18.06-S-Stress-Strain-attributes.csv

- C00Al6xxxT81_Numisheet2020R02T2.675W18.05-S
  C00Al6xxxT81Numisheet2020R02T2.675W18.05-S-Stress-Strain.csv
  C00Al6xxxT81Numisheet2020R02T2.675W18.05-S-Stress-Strain-attributes.csv

- C00Al6xxxT81_Numisheet2020R03T2.696W18.05-S
  C00Al6xxxT81Numisheet2020R03T2.696W18.05-S-Stress-Strain.csv
  C00Al6xxxT81Numisheet2020R03T2.696W18.05-S-Stress-Strain-attributes.csv

- C00Al6xxxT4_Numisheet2020R01T1.521W17.91-S
  C00Al6xxxT4Numisheet2020R01T1.521W17.91-S-Stress-Strain.csv
  C00Al6xxxT4Numisheet2020R01T1.521W17.91-S-Stress-Strain-attributes.csv

- C00Al6xxxT4_Numisheet2020R02T1.513W17.94-S
  C00Al6xxxT4Numisheet2020R02T1.513W17.94-S-Stress-Strain.csv
  C00Al6xxxT4Numisheet2020R02T1.513W17.94-S-Stress-Strain-attributes.csv

- C00Al6xxxT4_Numisheet2020R03T1.52W17.94-S
  `C00Al6xxxT4Numisheet2020R03T1.52W17.94-S-Stress-Strain.csv`
  `C00Al6xxxT4Numisheet2020R03T1.52W17.94-S-Stress-Strain-attributes.csv`

4.6 Analysis files

4.6.1 Output

A comma-separated value file that summarizes the test results, analysis, and conditions accompanies this report. Another file describes the attributes of that summary file:

- `Numisheet2020-tension-compression-summary.csv`
- `Numisheet2020-tension-compression-summary-attributes.csv`

Although Appendix 4.2 reports only the ε_{yy} noise floor, the underlying analysis computed the values for other strain and displacement measures. That data is attached in this report as the data file `noise-floor-noisefloor.csv`.

4.7 NCAL information

This report and data are archived as NCAL collate ID [L200327-WEL-001]. Engineering stress-strain diagrams are provided for reference only.

References

[1] ASTM International. Standard practice for verification of testing frame and specimen alignment under tensile and compressive axial force application. Standard E1012-14e1, ASTM International, W. Conshohocken, Pa, 2012. doi:10.1520/E1012-14E01.

[2] ASTM International. Standard test methods of compression testing of metallic materials at room temperature. Standard E9-19, ASTM International, W. Conshohocken, Pa, 2019. doi:10.1520/E0009-19.

[3] E. M. C. Jones and M. A. Iadicola, editors. *A Good Practices Guide for Digital Image Correlation*. International Digital Image Correlation Society, 2018. doi:10.32720/idics/gpg.ed1.

Table 3: File-naming convention for a strain profile or stress-strain curve.
Filename: C00FeDP1180_Numisheet2020R01T1.046W17.93-S.csv

Entry	Description
C	Test type: U=uniaxial, C=Tension/Compression
00	Angle to the rolling direction in degrees, limited to two digits
Fe	Major alloy component: Fe or Al
DP1180	Alloy type. DP1180, BM1-DP980, 6xxx-T81, or 6xxx-T4
_Numisheet2020	common to all files
RXX	Index of repeat test R01 or R02 or R03
T1.046	Specimen thickness in mm, rounded to three digits past decimal. In this case 1.046 mm
W17.93	Specimen width in mm, rounded to two digits past the decimal. In this case 17.93 mm.
-S	Indicates that the test is imaging on the side of the specimen.
.csv	File type identifier

Table 4: Column descriptions for the tension/compression summary table file.

Variable	Units	Type	Description
Material		Char	Material Descriptor
BakeID		Char	Describes annealing run on 6xxx-T81 material. Was written on each individual sheet
Angle	degrees	Real	Angle of the tensile axis relative to the rolling direction. 0 is longitudinal. 90 = transverse
w	mm	Real	Specimen width
t	mm	Real	Specimen thickness
Material		Char	describes heat treatment. Retained for compatibility with other scripts
DICanalysis		Char	which analysis got used
FirstImage		Integer	first image to process (sometimes the rigid-body-motion images come first, so you can't count on starting with image 0
LastImage		Integer	last image to process
NumisheetID		Char	Numisheet 2020 Material designation, per Tom Stoughton 2019-11-19 email
BMTestIndex		Char	2-charcter representation of the number of the test: "01" "02" "03" Used in constructing file name
IncrementalSwitch		Integer	index of image where analysis switched to incremental correlation
TestDate		Char	Test date in the format YYYY-MM-DD
eyyNoiseFloor	um/m	Real	Noise floor estimate for true strains in the y direction = abs(mean(ε_{yy}))+sd(ε_{yy})
exxNoiseFloor	um/m	Real	Noise floor estimate for true strains in the x direction = abs(mean(ε_{xx}))+sd(ε_{xx})
exyNoiseFloor	um/m	Real	Noise floor estimate for true shear strains in the xy direction = abs(mean(ε_{xy}))+sd(ε_{xy})

Table 5: Format of the last 6 columns of the local-strain files.

Column head	Description
Count	Image count
Time_0	Time from camera 0 in seconds
Time_1	Time from camera 1 in seconds
Displacement	Displacement data in mm scaled by DIC acquisition program at 8 mm/V
Force-Upper	force in N measured by the upper load cell scaled by the DIC acquisition program at 10 000 N/V
Force-Lower	force in N measured by the lower load cell scaled by DIC acquisition program at 10 000 N/V

Notes: (1) The forces measured by the load cells in the anti-buckling fixture were recorded in most tests, but are not included here.